

# Liquid Biopsy for Patient Characterization in Cardiovascular Disease: Verification against Markers of Cytochrome P450 and P-Glycoprotein Activities

Brahim Achour<sup>1,9,\*</sup> , Pauline Gosselin<sup>2,3,†</sup>, Jean Terrier<sup>2,3,4</sup>, Yvonne Gloor<sup>4</sup>, Zubida M. Al-Majdoub<sup>1</sup> , Thomas M. Polasek<sup>5,6,7</sup> , Youssef Daali<sup>3,4,8</sup>, Amin Rostami-Hodjegan<sup>1,5,†</sup>  and Jean-Luc Reny<sup>2,3,†</sup>

Precision dosing strategies require accounting for between-patient variability in pharmacokinetics together with subsequent pharmacodynamic differences. Liquid biopsy is a valuable new approach to diagnose disease prior to the appearance of clinical signs and symptoms, potentially circumventing invasive tissue biopsies. However, the possibility of quantitative grading of biomarkers, as opposed to simply confirming their presence or absence, is relatively new. In this study, we aimed to verify expression measurements of cytochrome P450 (CYP) enzymes and the transporter P-glycoprotein (P-gp) in liquid biopsy against genotype and activity phenotype (assessed by the Geneva cocktail approach) in 30 acutely ill patients with cardiovascular disease in a hospital setting. After accounting for exosomal shedding, expression in liquid biopsy correlated with activity phenotype for CYP1A2, CYP2B6, CYP2C9, CYP3A, and P-gp ( $r = 0.44-0.70$ ,  $P \leq 0.05$ ). Although genotype offered a degree of stratification, large variability (coefficient of variation (CV)) in activity (up to 157%) and expression in liquid biopsy (up to 117%) was observed within each genotype, indicating a mismatch between genotype and phenotype. Further, exosome screening revealed expression of 497 targets relevant to drug metabolism and disposition (159 enzymes and 336 transporters), as well as 20 molecular drug targets. Although there were no functional data available to correlate against these large-scale measurements, assessment of disease perturbation from healthy baseline was possible. Verification of liquid biopsy against activity phenotype is important to further individualize modeling approaches that aspire to achieve precision dosing from the start of drug treatment without the need for multiple rounds of dose optimization.

## Study Highlights

### WHAT IS THE CURRENT KNOWLEDGE ON THE TOPIC?

Liquid biopsy is currently used for early diagnosis of disease by identifying expressed genes associated with certain diseases in floating exosomes in plasma. Genotyping can sort patients into bands of functional activity of proteins involved in pharmacokinetics (PK) and pharmacodynamics.

### WHAT QUESTION DID THIS STUDY ADDRESS?

Can liquid biopsy be used for quantitative assessment of proteins that influence PK and address variations in the function of proteins within a given genotype?

### WHAT DOES THIS STUDY ADD TO OUR KNOWLEDGE?

Expression levels of hepatic enzymes and transporters in liquid biopsy correlate with established functional measurements of the corresponding proteins in patients with cardiovascular disease.

### HOW MIGHT THIS CHANGE CLINICAL PHARMACOLOGY OR TRANSLATIONAL SCIENCE?

This provides a means of patient characterization in relation to individual hepatic drug elimination capacity and allows selection of the optimal dose from the start of treatment using model-informed precision dosing.

<sup>1</sup>Centre for Applied Pharmacokinetic Research, School of Health Sciences, University of Manchester, Manchester, UK; <sup>2</sup>General Internal Medicine, Department of Medicine, Geneva University Hospitals, Geneva, Switzerland; <sup>3</sup>Geneva Platelet Group, Faculty of Medicine, University of Geneva, Geneva, Switzerland; <sup>4</sup>Clinical Pharmacology and Toxicology, Department of Anaesthesiology, Pharmacology, Intensive Care and Emergency Medicine, Geneva University Hospitals, Geneva, Switzerland; <sup>5</sup>Certara, Princeton, New Jersey, USA; <sup>6</sup>Department of Clinical Pharmacology, Royal Adelaide Hospital, Adelaide, South Australia, Australia; <sup>7</sup>Centre for Medicine Use and Safety, Monash University, Melbourne, Victoria, Australia; <sup>8</sup>Institute of Pharmaceutical Sciences of Western Switzerland, University of Geneva, Geneva, Switzerland; <sup>9</sup>Present address: Department of Biomedical and Pharmaceutical Sciences, College of Pharmacy, University of Rhode Island, Kingston, Rhode Island, USA. \*Correspondence: Brahim Achour (achour@uri.edu)

<sup>†</sup>These authors contributed equally as first authors.

<sup>†</sup>These authors contributed equally as last authors.

Received December 4, 2021; accepted February 27, 2022. doi:10.1002/cpt.2576

Between-patient variability in drug response is a significant challenge for healthcare providers, often leading to suboptimal clinical outcomes.<sup>1</sup> The requirement to cease therapy or change dosage regimens is highlighted by cases of adverse reactions and ineffective prescribed regimens. Initiatives that depart from a “one-size-fits-all” approach toward more individualized strategies require defining the principal patient characteristics that determine the fate of drugs in the body in order to optimize drug therapy using pharmacokinetic (PK) models. The definition of such factors will invariably include quantitative characterization of drug-metabolizing enzymes and transporters in relatively noninvasive alternatives to tissue biopsies.<sup>2</sup>

Several characterization approaches are currently implemented, which include genotyping of polymorphic genes (e.g., CYP2D6),<sup>3</sup> cocktails of exogenous substrates (e.g., the “Geneva cocktail”),<sup>4</sup> and measuring endogenous biomarkers (e.g., 4 $\beta$ -hydroxycholesterol-to-cholesterol ratio for CYP3A activity).<sup>5</sup> However, each of these has limitations. Genotyping offers a relatively non-quantitative indication of functional activities, exogenous substrates require administration of drugs to patients with inherent logistic challenges, and endogenous biomarkers are typically nonselective for specific metabolizing/transporter pathways.<sup>2</sup> Therefore, robust “liquid biopsy” assays have been proposed recently to complement, or even replace, such techniques.<sup>6,7</sup> Unlike blood-based assays used in diagnosis of cancer and other diseases,<sup>8,9</sup> techniques that monitor plasma-derived exosomal biomarkers of PK go beyond evidence of presence or absence (e.g., mutation profiles) to define a continuous quantitative grade as a proxy for a patient’s individual elimination capacity.<sup>6,7</sup> The advantages of this approach include its minimal invasiveness, routine accessibility of clinical samples, and the quantitative nature of the measurements, which offer a robust link with hepatic abundance of enzymes and transporters after accounting for liver-to-plasma shedding variability in individual patients.<sup>6,10</sup>

We previously reported a novel liquid biopsy assay and demonstrated its utility in assessing the hepatic abundance of pharmacologically relevant proteins in patients with liver cancer.<sup>6</sup> However, the link between liquid biopsy measurements and activity phenotypes is only available for small groups of individuals who had increased amounts of expressed proteins after induction.<sup>7,11</sup> Moreover, reported correlations are limited to two functional assays, midazolam 1-hydroxylation (CYP3A) and dextromethorphan O-demethylation (CYP2D6).<sup>11</sup> To further explore the potential clinical application of liquid biopsy for precision dosing, this study aimed to verify expression of CYP enzymes and the transporter P-gp in liquid biopsy against genotype and activity phenotype. The study was conducted in a population of inpatients with cardiovascular disease (CVD) with a set of samples characterized for activity of PK targets.

## METHODS

### Clinical samples and study design

The liquid biopsy experiments were performed on a subset of samples from the “Antithrombotics Therapeutic Optimization in Hospitalized Patients Using Physiologically and Population-based Pharmacokinetic Modeling” (OptimAT) study. OptimAT (Geneva University Hospitals, NCT03477331) is an observational prospective study on PK predictive models for optimization of antithrombotics. The study was approved by

the Ethics Committee of Geneva University Hospitals CCER (2017-00225), and samples were collected with prior informed consent. Patients received a range of drugs for CVD, including direct oral anticoagulants and/or antiplatelet drugs.

In this exploratory study, samples ( $n = 30$ ) were selected by the clinical team (Geneva University Hospitals) primarily based on CYP3A phenotype to represent a range of activity, according to a previously published classification.<sup>4</sup> Donors receiving known strong and moderate CYP3A inhibitors or major inducers were not eligible for inclusion in the subset. Samples were sorted according to relevant comorbidities and demographic characteristics (ethnicity, age, underlying conditions, and renal function) to ensure matching of covariates across the range of the selected set. The group conducting the liquid biopsy experiments and data analysis (the University of Manchester) were blinded to this information until the liquid biopsy results were available for comparison. Demographic and clinical details of the 30 donors are summarized in **Table 1** (detailed information is listed in **Tables S1, S2**). Healthy plasma from seven donors, used as control to establish baseline shedding and expression of targets, was supplied by BioIVT (West Sussex, UK; **Table S3**). The study design is summarized in **Figure 1**; genotype, activity phenotype, and liquid biopsy data were generated independently and the analysts on each side were blinded until all sets of data were available for statistical analysis.

### Measurement of the expression of CYP enzymes and P-gp in liquid biopsy

Plasma samples were processed to measure shedding and expression of cell-free RNA (cfRNA) of enzymes and transporters, as previously described.<sup>6</sup> Briefly, exosomes were extracted from individual platelet-depleted EDTA-plasma samples ( $n = 30$ , volume 0.50–0.97 mL) by polymer-assisted precipitation (ExoQuick; System Biosciences, Palo Alto, CA) and gentle centrifugation (1500 g, 60 minutes at 4°C). Total cfRNA was extracted using MagMax cell-free total nucleic acid isolation kit (Thermo Fisher Scientific, Austin, TX). One sample failed at this stage. Extracted RNA was assessed on a 2100 Bioanalyzer Desktop System (Agilent, Santa Clara, CA) with RNA 6000 Pico kit (Agilent) to evaluate RNA yield and quality (DV200 score: percentage of fragments > 200 nt relative to total RNA).

Reverse transcription was performed with 3.5  $\mu$ L of cfRNA using AmpliSeq cDNA Synthesis for Illumina (Illumina, Cambridge, UK), and the resultant cDNA (5  $\mu$ L) was used in target amplification by polymerase chain reaction (PCR; 16 cycles) using Illumina’s AmpliSeq Transcriptome Human Gene Expression Panel and AmpliSeq HiFi Mix, part of AmpliSeq Library PLUS (96 reactions). Amplicon libraries were purified and further amplified (7 cycles), followed by normalization (2 nM), dilution (400 pM), and pooling. Pooled libraries were sequenced on a NovaSeq 6000 platform (Illumina) with 2  $\times$  150 bp paired end reads using NovaSeq 6000 S2 Reagent kit (300 cycles). Each clinical sample was prepared in duplicate and one replicate was sequenced twice (providing a total of 92 replicates; **Figure S1**). To establish baseline expression and shedding, the same methods were applied to plasma from healthy donors ( $n = 7$ , volume 1–3 mL).

Sequencing data were processed using RNA Amplicon App 2.0.1 (Illumina) and the Burrows Wheeler Aligner. Differential expression analysis used the DESeq2 algorithm<sup>12</sup> to generate expression data for the targets (enzymes and transporters) and liver-specific markers (APOA2, FGB, AHSB, HPX, SERPINC1, F2, CFHR2, F9, SPP2, MBL2, A1BG, TF, and C9) that make up the liver-to-plasma shedding factor used to offset variability in shedding of liver exosomes (**Figure S2**), as previously defined.<sup>6,10</sup> The core set of targets was selected to reflect the phenotype range (CYP1A2, CYP2B6, CYP2C9, CYP2C19, CYP2D6, CYP3A4/5/7, and ABCB1), and a cutoff value of  $\geq 3$  reads per transcript was used to ensure reliable quantification. To minimize bias related to variable sample volume (and yield), expression levels were normalized to the total number

**Table 1 Summary of patient characteristics**

Characteristics	Mean ± SD (range) or number
Age, years	66 ± 5 (60–75)
Sex	7 female, 23 male
Height, cm	173 ± 9 (150–197)
Body weight, kg	82 ± 16 (50–120)
BMI, kg/m <sup>2</sup>	27 ± 5 (16–41)
Liver function	
ASAT (U/L)	31 ± 17 (10–73)
ALAT (U/L)	32 ± 23 (10–127)
GGT (U/L)	80 ± 101 (16–526)
ALP (U/L)	118 ± 246 (33–1406)
Bilirubin, μmol/L	10 ± 6 (3–26)
Renal function	
eGFR, mL/min/1.73 m <sup>2a</sup>	80 ± 17 (41–106)
Creatinine clearance, mL/min <sup>b</sup>	85 ± 23 (0.3–119)
Tobacco and alcohol	
Current smoker	7
Drinker	12
Main comorbidities	
Atrial fibrillation	11
Chronic and acute heart failure	9
Chronic and acute coronary heart disease	17
Venous thromboembolism	8
Stroke	7
Type 2 diabetes	6
Cirrhosis	2
Obesity	5
Cancer <sup>c</sup>	6
Inflammatory/autoimmune disease <sup>d</sup>	2

ALAT, alanine aminotransferase; ALP, alkaline phosphatase; ASAT, aspartate aminotransferase; BMI, body mass index; GGT, gamma-glutamyl transferase.

<sup>a</sup>The eGFR was calculated using the Chronic Kidney Disease Epidemiology Collaboration (CKD-EPI) equation.

<sup>b</sup>The creatinine clearance was calculated using Cockcroft-Gault equation.

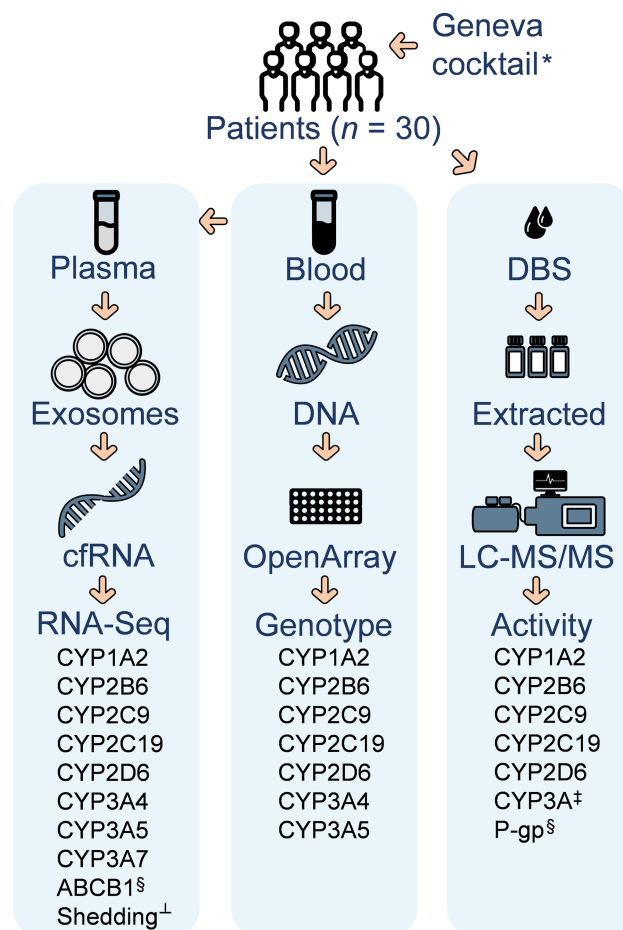
<sup>c</sup>The cancer diagnosis was prostate (*n* = 2), genito-urinary (*n* = 1), lung (*n* = 1), gastro-intestinal (*n* = 1), or hematologic cancer (*n* = 1).

<sup>d</sup>Inflammatory conditions were either rheumatoid arthritis with ankylosing spondylitis (*n* = 1) or Still's disease (*n* = 1).

of reads in each sample and recorded in units of reads per million (RPM). Further, the computed shedding factor was used for normalization of the levels of target enzymes/transporters, as detailed previously.<sup>6</sup>

### Activity phenotyping of CYP enzymes and P-gp

Activity phenotype was determined for six CYP enzymes (CYP1A2, CYP2B6, CYP2C9, CYP2C19, CYP2D6, and CYP3A) and P-gp in the same 30 patients, as previously described in detail.<sup>4,13</sup> Briefly, probe substrates in the Geneva cocktail (caffeine 50 mg, CYP1A2; bupropion 20 mg, CYP2B6; flurbiprofen 10 mg, CYP2C9; omeprazole 10 mg, CYP2C19; dextromethorphan 10 mg, CYP2D6; and midazolam 1 mg, CYP3A)<sup>4</sup> were orally administered to the patients. Capillary blood was collected 2, 3, and 6 hours post administration



\*Substrates: caffeine, bupropion, flurbiprofen, omeprazole, dextromethorphan, midazolam & fexofenadine

‡ The substrate midazolam is metabolized by CYP3A subfamily

§P-gp is the protein encoded by the ABCB1 gene

<sup>†</sup>Shedding is based on liver-specific markers: APOA2, FGB, AHSG, HPX, SERPINC1, F2, CFHR2, F9, SPP2, MBL2, A1BG, TF & C9

**Figure 1** Outline of the study. A total of 30 participants with cardiovascular disease were administered the Geneva cocktail orally. Blood samples were taken at 2, 3, and 6 hours post administration. The assessment of expression of liquid biopsy derived exosomal cell-free RNA (cfRNA) was carried out using Ampliseq RNA sequencing technology. Genotype determination was based on genomic DNA from blood using OpenArray technology. Activity phenotype was assessed in capillary DBS by extraction of substrate drugs and their metabolites from the filter paper and subsequent LC-MS/MS measurement. cfRNA, cell-free RNA; DBS, dried blood spots; LC-MS/MS, liquid chromatography–tandem mass spectrometry.

and dried blood spots were stored at  $-20^{\circ}\text{C}$  until analysis. The drugs and their CYP-specific metabolites were measured using a validated reversed-phase high performance liquid chromatography–tandem mass spectrometry method in dual electrospray ionization mode, as previously described.<sup>14</sup> Phenotypic classification was based on metabolic ratio (the concentration of the metabolite relative to the concentration of the substrate) at 2 hours post administration. Area under the curve (AUC) ratios were calculated using a noncompartmental analysis for a subset of donors (*n* = 23) based on three data points (2, 3, and 6 hours). In addition, oral fexofenadine (25 mg) was co-administered

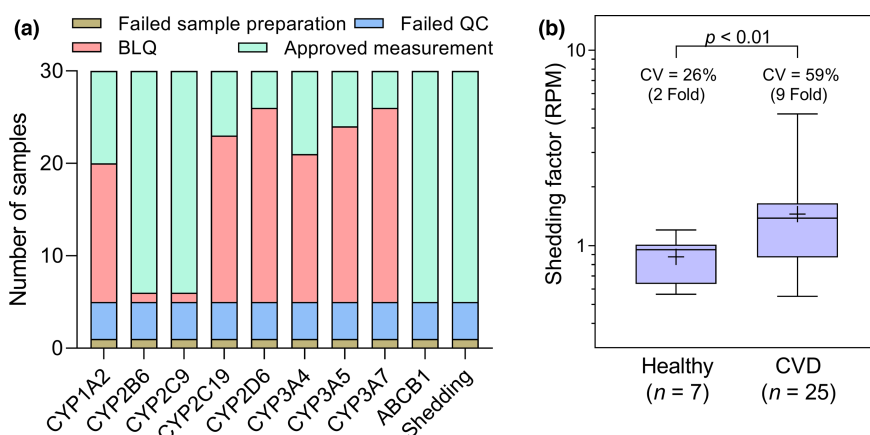


**Figure 2** Assessment of liquid biopsy RNA-Seq measurements in the CVD samples ( $n = 30$ ). (a) Quality assessment of liquid biopsy measurements; five samples failed either sample preparation or QC at the cDNA or sequencing stage, resulting in a maximum of 25 readouts per target enzyme/transporter. A proportion of the measurements were BLQ. (b) Liver-specific shedding was measured in all CVD samples that passed QC ( $n = 25$ ) and compared with shedding in healthy donors ( $n = 7$ ), which reflected higher and more variable shedding in the disease cohort. In parentheses is the maximum-to-minimum fold difference in shedding in each cohort. In **b**, the whiskers represent the range, the boxes are the 25th and 75th percentiles, the lines are the medians and the + signs are the means. BLQ, below the limit of quantification; CV, coefficient of variation; CVD, cardiovascular disease; QC, quality control; RPM, reads per million.

for P-gp phenotyping; drug concentration was determined 2, 3, and 6 hours post administration.

### Genotyping of CYP enzymes

Genotyping of CYP (1A2, 2B6, 2C9, 2C19, 2D6, 3A4, and 3A5) enzymes was performed as previously described.<sup>13,15</sup> Briefly, extraction of genomic DNA from PaxGene blood DNA tubes (Qiagen, Hombrechtikon, Switzerland) was carried out using QIAasympyony DNA blood midi kit (Qiagen), followed by genotyping using TaqMan OpenArray PGx Express Panels (Life Technologies Corporation, Carlsbad, CA) performed on a QuantStudio 12K Flex real time PCR System (Thermo Fisher Scientific, Rochester, NY). Single nucleotide polymorphisms used to assess the CYP genotypes are listed in Table S4. CYP2D6 gene duplication or deletion was assessed with TaqMan Copy Number Assay Hs00010001 with RNase P as a reference (Thermo Fisher Scientific). Translation of genetic patterns to pharmacogenomic star allele nomenclature was done using translational tables (Thermo Fisher Scientific and PharmGKB).<sup>16</sup>

### Statistics and data analysis

Exosome RNA sequencing data were included in the analysis only for samples that had (i) sufficient cfRNA yield ( $> 1$  ng/mL) and quality (DV200 score  $> 20\%$ ), (ii) visible cDNA peak at approximately 280 bp in amplicon preparations, (iii) sufficient transcriptome sequencing depth (total  $> 10$  M reads), and (iv) a number of reads for each target above the cutoff limit ( $\geq 3$  reads). Replicate measurements were averaged. The locally weighted scatterplot smoothing (LOESS) regression and Pearson correlation were applied to assess the relationship between phenotype (activity) and liquid biopsy data (expression) in the CVD sample set. Assessment of correlations only included targets (CYP enzymes and P-gp) that had data coverage of  $> 25\%$  of the samples (i.e.,  $> 7$  samples). Activity of CYP3A was assessed against combined expression of CYP3A4/5/7, taking into consideration CYP3A5 genotype. Differences (in activity, shedding, and expression) between groups (disease, genotype, sex, and age) were assessed using a two-tailed unpaired *t*-test with Welch's correction for inequivalent variance. Differences across several groups (genotype and body mass index) were assessed with analysis of variance (ANOVA) with Welch's correction. A *P* value cutoff of 0.05 was considered for statistical significance. Data analysis and visualization were carried out using Microsoft Excel 2016, GraphPad Prism 9.1.2 (GraphPad Software, La Jolla, CA) and R software version 4.1.2.

## RESULTS

Samples from the same set of patients were characterized by three methods independently: genotyping, activity phenotyping, and expression in liquid biopsy (Figure 1). The analysis examined relationships among these three approaches. Additional information from liquid biopsy screening of targets, which had no available functional data or genotype, was assessed separately.

### Expression of enzymes and transporters in liquid biopsy

The yield of cfRNA was  $4.95 \pm 3.85$  ng/mL plasma, with a quality (DV200) score of  $54\% \pm 15\%$ , indicating moderate yield and good quality of extracted exosomal RNA. AmpliSeq aimed to sequence  $> 20,000$  human RefSeq genes per sample, generating an average of 32.06 million reads per sample. Sequencing quality was excellent, with  $> 96\%$  of sequenced bases achieving a sequencing quality score (Q-score) of  $\geq 30$  (i.e.,  $\geq 99.9\%$  base call accuracy). Out of the 30 CVD samples, 25 samples passed quality control at the RNA, cDNA and sequencing levels (Figure 2a). The number of transcripts measured in the CVD sample set ranged from 14,747 to 21,021 (average  $19,285 \pm 1,321$  per sample). This allowed quantification of 497 genes related to drug PK, which included 159 enzymes, 336 transporters, and the neonatal Fc receptor (FcRn)  $\alpha$ - and  $\beta$ -subunits (Table S6). Disease perturbation of PK targets in CVD samples from baseline expression in healthy donors ( $n = 7$ ) was defined, with change ranging from 0.1 to 18-fold, whereas 10 PK targets were quantifiable only in the disease cohort. A total of 124 PK targets (25%) exhibited disease-related differential expression (Table S6 shows a list of quantified PK targets with perturbation data).

### Normalized expression of CYP enzymes and P-gp against liver shedding

Liver-specific markers were measured to determine patient-specific liver shedding into the bloodstream. Shedding was moderately, but statistically significantly, higher and more variable in

patients with CVD ( $1.45 \pm 0.86$  RPM) than in healthy donors ( $0.87 \pm 0.23$  RPM; Welch's *t*-test,  $P < 0.01$ ; **Figure 2b**), and large differences were observed between shedding in CVD and previously reported levels in liver cancer<sup>6</sup> ( $P < 0.001$ ; **Figure S2c**). Sex, smoking, and drinking had little impact on shedding in the study cohort ( $P > 0.05$ ), whereas levels fluctuated with age in older adults (higher in 60–69 year old donors compared with their 70–75 year old counterparts,  $P = 0.02$ ). Shedding was 40%–50% higher in overweight and obese patients compared with those with a healthy body mass index (following established clinical classification), but differences did not reach statistical significance (Welch's ANOVA,  $P = 0.14$ ; **Figure S3**). Shedding-normalized expression data for CYP enzymes and ABCB1/P-gp are summarized in **Table 2** and **Figure 3a**. The technique distinguished between three CYP3A (4/5/7) isoforms, which had a combined activity phenotype. Variability (coefficient of variation (CV)) in expression of these targets in the CVD cohort ranged from 54% to 125%.

### Activity phenotype of CYP enzymes and P-gp

Activity phenotype was determined for six CYP enzymes and P-gp using the Geneva cocktail; concentration (ratio) and AUC (ratio)

data are summarized in **Table 2** and **Figure 3b**. The activities of CYP enzymes were determined as metabolic ratios (2 hours) and AUC ratios (2, 3, and 6 hours) for 30 and 23 samples, respectively. In the case of P-gp, the concentration and AUC of fexofenadine in 30 and 23 samples, respectively, were used instead. Concentration (ratio) and AUC (ratio) data were highly correlated ( $R^2 = 0.66$ – $0.99$ ,  $P < 0.001$ , for CYP enzymes, and  $R^2 = 0.87$ ,  $P < 0.001$ , for P-gp; **Figure S4**). Variability (CV) in activity phenotype ranged from 42% to 204% in concentration data and 36% to 203% in AUC data.

### Assessment of expression and activity of CYP enzymes against their genotype

Genotype of CYP1A2, 2B6, 2C9, 3A4, and 3A5 was determined for all patients ( $n = 30$ ), whereas genotype of CYP2C19 and 2D6 was determined for 29 and 27 patients, respectively (**Table S5**). Comparison of expression and activity across genotype groups revealed a range of variabilities (CV) in each genotype bracket (37%–117% in expression; 16%–157% in activity), with considerable overlap in both types of measurement (**Figure 4**). Differences in activity were significant across genotypes in the cases of CYP2C9 (ANOVA,  $P < 0.01$ ) and CYP2C19 (ANOVA,  $P < 0.05$ ), confirming the expected reduced function of \*2 and \*3 allele products

**Table 2** Genotype, expression in liquid biopsy and activity phenotype of CYP enzymes and P-gp

Gene/protein	Genotype <sup>a</sup>	Expression in liquid biopsy <sup>b</sup>	Activity phenotype <sup>c</sup>	
			MR ([metabolite] <sub>2 hours</sub> /[drug] <sub>2 hours</sub> )	AUCR (AUC <sub>metabolite</sub> /AUC <sub>drug</sub> )
CYP1A2	*1/*1 (100%)	0.46 ± 0.40 (0.07–1.31)	0.28 ± 0.12 (0.07–0.57)	0.33 ± 0.15 (0.08–0.67)
CYP2B6	*1/*1 (83.3%); *1/*5 (10%); *1/*22 (3.3%); *5/*5 (3.3%)	0.64 ± 0.80 (0.03–3.43)	2.66 ± 2.86 (0.04–12.96)	4.63 ± 4.70 (0.98–22.77)
CYP2C9	*1/*1 (66.7%); *1/*2 (16.7%); *1/*3 (13.3%); *2/*3 (3.3%)	2.34 ± 2.59 (0.05–10.68)	0.10 ± 0.04 (0.02–0.24)	0.09 ± 0.03 (0.05–0.17)
CYP2C19	*1/*1 (40%); *1/*2 (13.3%); *1/*17 (36.7%); *2/*17 (6.7%); ND (3.3%)	1.13 ± 1.10 (0.24–3.35)	0.42 ± 0.86 (0.05–4.20)	0.45 ± 0.91 (0.05–4.06)
CYP2D6	*1/*1 (27.7%); *1/*2 (13.3%); *1/*4 (6.7%); *1/*41 (13.3%); *2/*2 (10.0%); *2/*2x2 (3.3%); *2/*4 (6.7%); *2/*5 (3.3%); *2/*9 (3.3%); *4/*41 (3.3%); ND (10.0%)	0.27 ± 0.14 (0.11–0.43)	1.68 ± 1.06 (0.11–3.70)	1.48 ± 0.95 (0.09–3.48)
CYP3A4	*1/*1 (93.3%); *1/*22 (6.7%)	0.21 ± 0.18 (0.02–0.54)	0.68 ± 0.50 (0.08–2.00) <sup>d</sup>	0.64 ± 0.49 (0.14–1.73) <sup>d</sup>
CYP3A5	*1/*3 (10%); *3/*3 (90%)	0.25 ± 0.20 (0.02–0.61)		
CYP3A7	-	0.20 ± 0.24 (0.02–0.55)		
			Concentration (ng/mL)	AUC (ng·h/mL)
ABCB1/P-gp	-	23.72 ± 24.86 (2.76–96.52)	43.04 ± 22.70 (12.0–95.40)	179.70 ± 95.49 (43.50–389.00)

AUC, area under the curve; AUCR, area under the curve ratio; MR, metabolic ratio; ND, not determined; - Symbols indicate unavailable data.

<sup>a</sup>The determined genotype and percentage of samples in each genotype group (out of  $n = 30$ ).

<sup>b</sup>Liquid biopsy expression in plasma-derived exosomes reported as mean ± SD (range) in units of reads per million (RPM).

<sup>c</sup>Activity phenotype determined in capillary dried blood spots (DBS) and reported as mean ± SD (range). For CYPs, MR is the metabolite concentration to drug concentration at time 2 hours and AUCR is the AUC ratio of metabolite to drug based on three time points (2, 3, and 6 hours). Measured metabolite/drug pairs were paraxanthine/caffeine (CYP1A2), OH-bupropion/bupropion (CYP2B6), OH-flurbiprofen/flurbiprofen (CYP2C9), OH-omeprazole/omeprazole (CYP2C19), dextrorphan/dextromethorphan (CYP2D6), and OH-midazolam/midazolam (CYP3A). For P-gp, fexofenadine concentration and AUC were measured.

<sup>d</sup>Activity phenotype of CYP3A.

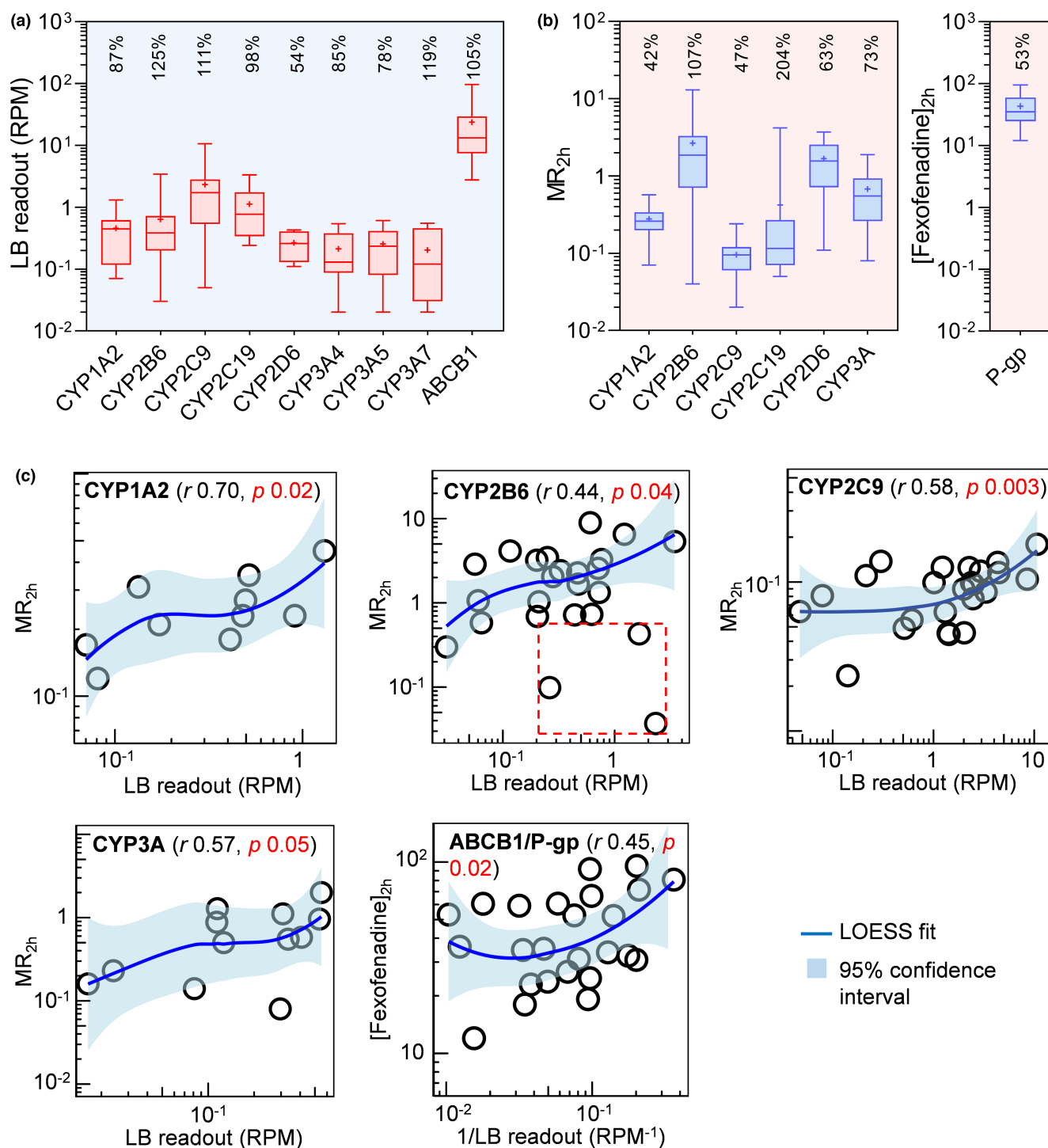


**Figure 3** Assessment of liquid biopsy expression and activity phenotype of CYP enzymes and P-gp in patient samples ( $n = 30$ ). The assessment was based on (a) quantification of the RNA expression of CYP enzymes and ABCB1 in plasma-derived exosomes and (b) measurement of activity of the corresponding proteins (CYP enzymes and P-gp) in dried blood spots against the Geneva cocktail. Expression was normalized to shedding and activity was measured at 2 hours post cocktail administration. In a and b, the whiskers represent the range, the boxes are the 25th and 75th percentiles, the lines are the medians and the + signs are the means. The percentages above the data are the coefficients of variation. (c) Correlations were assessed for five targets that returned a sufficient number of data points above the limit of quantification in liquid biopsy (> 25% of samples). In c, the dashed box (CYP2B6 correlation) encloses outlier readouts. LB, liquid biopsy; LOESS, locally weighted scatterplot smoothing; MR, metabolic ratio; RPM, reads per million.

(Table S5). Limited differences between activities of CYP2D6 genotype groups were observed, consistent with the predicted activity scores (20 out of 27 genotyped samples were predicted to

have normal activity; Table S5). Expression mirrored the pattern observed with CYP2C9 activity, but differences did not reach statistical significance.

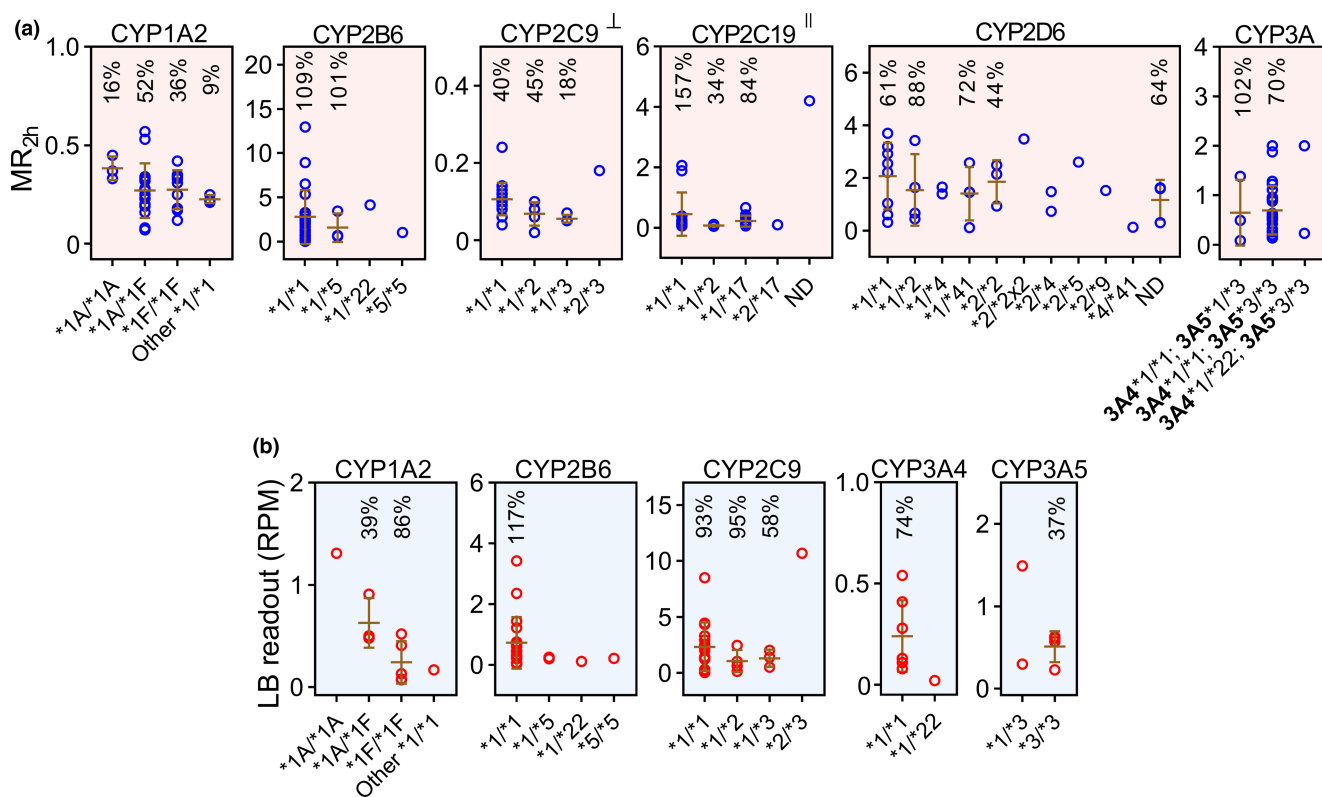


**Figure 4** Assessment of (a) activity phenotype and (b) expression in liquid biopsy against genotype of CYP enzymes in patient samples ( $n = 30$ ). The genotype was determined for CYPs 1A2, 2B6, 2C9, 2C19, 2D6, 3A4, and 3A5. Activity measurements were carried out in dried blood spots against the Geneva cocktail. Liquid biopsy measurements were based on quantification of RNA expression in plasma-derived exosomes. Data are only shown for enzymes with a sufficient number of measurements (at least 3 measurements in at least one genotype group). The lines are the means, the error bars are SD values, and the numbers above the data points are the coefficients of variation of measurements corresponding to each genotype where there were  $\geq 3$  measurements. Comparisons were done using ANOVA or a  $t$ -test with Welch's correction for unequal variance:  $^{\dagger}p < 0.05$ ,  $^{\ddagger}p < 0.01$ . In **a**, activity of CYP3A does not correspond to a specific isoform, and is assessed against a combined genotype annotation for CYP3A4 and CYP3A5. ANOVA, analysis of variance; LB, liquid biopsy; MR, metabolic ratio; ND, not determined; RPM, reads per million.

### Correlation of CYP and P-gp expression in liquid biopsy with activity phenotype

Correlations between measurements of activity and liquid biopsy expression of CYP1A2, CYP2C9, CYP3A, and ABCB1/P-gp were moderate to strong ( $r = 0.45$ – $0.70$ ,  $P \leq 0.05$ ; **Figure 3c**). The correlation of CYP2B6 was moderate and relatively more complicated because of outliers relating to patients on a strong CYP2B6 inhibitor, clopidogrel,<sup>17</sup> which affects activity without interfering with expression ( $r = 0.44$ ,  $P = 0.04$ ; **Figure 3c**). Similar relationships were uncovered with replicate liquid biopsy measurements against activity data (**Figure S5**). Correlating CYP2C19 and CYP2D6 expression and activity data was not possible due to the low number of data points; these two enzymes returned several expression measurements below the limit of quantification (**Figure 2a**).

### Exploratory screening of expression of molecular drug targets in liquid biopsy

The patients received a range of medications for the management of CVD, including antihypertensive, lipid-lowering, antithrombotic, antiplatelet, and antidiabetic drugs. Liquid biopsy enabled monitoring variability in the expression of the pharmacodynamic (PD) targets of these drugs (**Table S7**). Unlike PK targets

(specific expression, particularly in the liver, intestine, and kidneys; **Table S6**), drug targets are typically ubiquitously expressed and not specific to any particular tissue, and, therefore, their expression was normalized to total RNA shed by the whole organism into the bloodstream, (cRNA<sub>TOTAL</sub>), measured in each plasma sample. Variability (CV) in the 20 monitored PD targets ranged from 22% to 110%, which is similar to the range of variability observed for drug-metabolizing enzymes and transporters. Disease perturbation of PD targets in CVD samples from baseline expression in healthy donors ( $n = 7$ ) ranged from 0.7 to 4-fold (**Table S7**). One PD target (MT-ND3), related to the mode of action of metformin, was not detected because it is encoded by a mitochondrial gene, whereas the reported liquid biopsy technique quantifies expression of genomic DNA.

### DISCUSSION

New drugs are tested predominantly in uniform cohorts of healthy subjects or patients during each clinical phase of drug development,<sup>18</sup> and many patients are excluded from such studies by default without a scientific rationale, according to a recent US Food and Drug Administration (FDA) Guidance document.<sup>19</sup> Hence, changes in dose recommendations for different subpopulations of

patients are common in clinical practice after regulatory approval.<sup>18</sup> The published FDA Guidance aimed to encourage broadening eligibility criteria and increasing diversity in clinical trials by enrolling patients from under-represented subpopulations.<sup>19</sup> However, implementation of this guidance will inevitably require defining the changes that occur in relevant PK pathways in patients prior to their enrollment. Although liver biopsies are invasive and impractical for routine clinical use, tissue proteomics-informed PK modeling was recently deployed to achieve precise dosing in a cohort of obese patients,<sup>20</sup> highlighting the utility of a systems pharmacology approach for precision dosing. To overcome the bottleneck of invasive sampling, newly developed liquid biopsy-based exosomal techniques<sup>6,7,21</sup> were proposed as a more practical and routinely accessible alternative to tissue biopsies. We previously reported a liquid biopsy-based assay for patient characterization, which takes advantage of state-of-the-art exosome and sequencing technologies to afford a quantitative measurement of individual drug elimination capacity.<sup>6,10</sup> Whereas a link was established between liquid biopsy measurements and the amounts of the corresponding proteins in matching liver tissue, there was no indication as to whether the approach would work in real-world samples from a hospital setting or whether measurements would compare to established functional assays of activity. Herein, we report further assessment of the liquid biopsy assay against genotype and activity phenotype, focusing on CYP enzymes and P-gp as a core set of targets, given their key role in determining drug PK. The study focused on a cohort of inpatients with CVD, characterized for activity of PK targets. These patients suffer from different comorbidities as well as inflammatory conditions and are susceptible to varying levels of drug interactions due to polypharmacy. Therefore, this population is representative of patients who may benefit from precise dosing.<sup>22</sup>

Although the role of pharmacogenomics in precision dosing is emphasized by genetic variations that affect the activity of polymorphic genes, assessment of genotype against expression/activity phenotype confirmed previous observations of wide variability within each genotype and extensive overlap across genotypes.<sup>3,23</sup> The cases of highly polymorphic enzymes were no exception (CYP2D6, CYP2C9, and CYP2C19 in this study). In particular, the reported large variability in the activity and expression of CYP3A4,<sup>24</sup> the most clinically relevant CYP enzyme for metabolic clearance, cannot be explained by genetics (24-fold variability in expression of CYP3A4\*1/\*1 in the present study). Therefore, pharmacogenomics is insufficient, at least independently, for individualized characterization of patients' drug handling capacity. Rather, a quantitative measure, such as expression or activity, is required. To this end, the correlations between quantitative measurements offered by activity phenotyping and liquid biopsy technology are promising. These relationships support and expand on previously reported liquid biopsy work that focused on relative changes in CYP3A4 following induction by rifampicin in healthy volunteers<sup>7</sup> and in CYP3A4 and CYP2D6 in subjects with naturally induced levels (pregnancy) compared with noninduced expression.<sup>11</sup> We not only assessed patients from a hospital setting but also determined variability at base level and for several targets. A roadmap to application of such data with PK modeling for model-informed precision dosing (MIPD) was outlined previously<sup>2</sup>; liquid biopsy data are applicable in both population PK and physiologically-based pharmacokinetic

(PBPK) approaches, by enabling characterization of the metabolic and transport pathways in individual patients, especially in the extreme cases of potential toxicity or lack of pharmacological effect.

Liquid biopsy measurements were normalized for variation in liver-to-plasma shedding (comprising variability in 13 liver markers), as described previously.<sup>6</sup> We confirmed that shedding is population-specific,<sup>6,10</sup> and therefore comparison of different patient groups based on non-corrected measurements in liquid biopsy might bias the assessment. Accounting for shedding is especially important to establish a link with organ function in progressive disease where there is a wide distribution of exosomal yield.<sup>6,25–27</sup> Projected expression of target proteins in the relevant organ (liver in this case) based on liquid biopsy data can be used to complement genotype/phenotype information as described before.<sup>2</sup> However, there are advantages to implementing projected expression values in the organ from the liquid biopsy output over activity measures by cocktails. Although both apply to a series of drugs with multiple elimination pathways and variable contributions of each pathway to overall exposure, liquid biopsy covers a much broader range of pathways compared with cocktails, which are limited in their scope to a handful of targets in each cocktail. Indeed, exosome screening allowed monitoring of a large number of PK targets (159 enzymes, 336 transporters and FcRn), consistent with our previous work,<sup>6</sup> and recovered disease perturbation in their expression from healthy baseline, revealing differential expression in approximately a quarter of PK targets. The screening also allowed monitoring of 20 molecular targets of the CVD medications received by the patients, including targets of antithrombotic, antiplatelet, lipid-lowering, antidiabetic, and antihypertensive drugs. Disease perturbation to PD targets was not as clear-cut as PK targets because of the heterogeneous range of pathologies in CVD and the limited sample size; for example, nine patients had heart failure, six had diabetes, and five were obese. Therefore, probing changes in drug targets in the whole cohort did not reveal drastic changes from healthy baseline. To our knowledge, this is the first report of monitoring FDA-approved molecular drug targets in plasma exosomes from acutely ill patients with CVD. Individual expression and disease perturbation data are essential system parameters for building "Virtual Twin" models within an MIPD framework.<sup>1,28</sup>

One limitation of the study was the low coverage of several targets in the liquid biopsy data, particularly CYP2D6 and CYP2C19. This highlights the technical challenges that preclude the widespread use of liquid biopsy beyond research. The attrition rate in the CVD samples confirmed the importance of collecting a large volume of good quality plasma (at least 1 mL), with the current technical constraints, to achieve sufficient exosomal yield to quantify poorly expressed targets. By contrast, all healthy samples in the current study and cancer samples in our previous report<sup>6</sup> passed quality control owing to their larger volumes (especially in the case of healthy samples) and higher shedding (in the case of the cancer cohort). In addition, two specific aspects of the liquid biopsy technique were evident. First, inhibitors, which do not necessarily affect protein expression, lead to a mismatch between phenotype and liquid biopsy results. This disconnect was observed with strong inhibition of CYP2B6 by clopidogrel.<sup>17</sup> Although this



may be considered a shortfall, liquid biopsy provides information on multiple pathways, and the generated data should characterize the kinetics of the inhibitor as well as the substrate. This allows description of the level of inhibition using concentration-time profiles of the inhibitor with PBPK models.<sup>29</sup> It is worth noting that inhibition that leads to suppression of expression, such as that due to inflammatory factors (e.g., interleukin 6 (IL-6)),<sup>30</sup> should not cause such mismatch between activity and liquid biopsy data. Further, genes encoding proteins with structural or functional defects (e.g., CYP3A5\*3) are transcribed to mRNA and sometimes translated to protein, both of which are detectable in liquid biopsy while being inactive or having compromised activity against their substrates. Therefore, interpretation of measurements requires additional knowledge about the patients and their medications to support more accurate determination of drug elimination capacity.

In conclusion, the correlation data presented herein further support using liquid biopsy as a patient characterization approach applicable for precision dosing. Although complementary information from genotyping and phenotyping is highlighted, the remarkable range of PK and PD targets simultaneously monitored in liquid biopsy offers a strong basis for populating individualized models with the required system data. The liquid biopsy approach for quantitative assessment of different targets related to precision dosing is understandably in its early stages with many unknowns. Nonetheless, with trends toward individualization of treatment,<sup>2</sup> liquid biopsy provides an unrivalled opportunity for the creation of digital replicates of patients for the purpose of enabling MIPD.<sup>28</sup>

#### ACKNOWLEDGEMENTS

The authors thank Illumina (Cambridge, UK) for access to sequencing facilities.

#### SUPPORTING INFORMATION

Supplementary information accompanies this paper on the *Clinical Pharmacology & Therapeutics* website ([www.cpt-journal.com](http://www.cpt-journal.com)).

#### FUNDING

This study was supported by the Centre for Applied Pharmacokinetic Research (CAPKR) consortium (Eli Lilly, Takeda, Genentech, AbbVie, Merck-Serono, MSD, GSK, Servier, and Janssen).

#### CONFLICT OF INTEREST

Certara holds several patents related to Liquid Biopsy, and T.M.P., A.R.-H. (via employment), and B.A. (via consultancy) are linked to Certara's activities in this space. All other authors declared no competing interests for this work.

#### AUTHOR CONTRIBUTIONS

B.A., P.G., J.T., Y.G., T.M.P., Y.D., A.R.-H., and J.-L.R. wrote the manuscript. B.A., T.M.P., Y.D., A.R.-H., and J.-L.R. designed the research. B.A., P.G., J.T., Y.G., and Z.M.A. performed the research. B.A., P.G., J.T., Y.G., Y.D., A.R.-H., and J.-L.R. analyzed the data.

© 2022 The Authors. *Clinical Pharmacology & Therapeutics* published by Wiley Periodicals LLC on behalf of American Society for Clinical Pharmacology and Therapeutics

This is an open access article under the terms of the [Creative Commons Attribution-NonCommercial](https://creativecommons.org/licenses/by-nc/4.0/) License, which permits use, distribution and reproduction in any medium, provided the original work is properly cited and is not used for commercial purposes.

- Polasek, T.M., Shakib, S. & Rostami-Hodjegan, A. Precision dosing in clinical medicine: present and future. *Expert Rev. Clin. Pharmacol.* **11**, 743–746 (2018).
- Darwich, A.S. et al. Model-informed precision dosing: background, requirements, validation, implementation, and forward trajectory of individualizing drug therapy. *Annu. Rev. Pharmacol. Toxicol.* **61**, 225–245 (2021).
- Gaedigk, A. et al. The CYP2D6 activity score: translating genotype information into a qualitative measure of phenotype. *Clin. Pharmacol. Ther.* **83**, 234–242 (2008).
- Bosilkovska, M. et al. Geneva cocktail for cytochrome P450 and P-glycoprotein activity assessment using dried blood spots. *Clin. Pharmacol. Ther.* **96**, 349–359 (2014).
- Diczfalusy, U., Nylén, H., Elander, P. & Bertilsson, L. 4 $\beta$ -Hydroxycholesterol, an endogenous marker of CYP3A4/5 activity in humans. *Br. J. Clin. Pharmacol.* **71**, 183–189 (2011).
- Achour, B. et al. Liquid biopsy enables quantification of the abundance and interindividual variability of hepatic enzymes and transporters. *Clin. Pharmacol. Ther.* **109**, 222–232 (2021).
- Rowland, A. et al. Plasma extracellular nanovesicle (exosome)-derived biomarkers for drug metabolism pathways: a novel approach to characterize variability in drug exposure. *Br. J. Clin. Pharmacol.* **85**, 216–226 (2019).
- Lanman, R.B. et al. Analytical and clinical validation of a digital sequencing panel for quantitative, highly accurate evaluation of cell-free circulating tumor DNA. *PLoS One* **10**, e0140712 (2015).
- Gupta, R. et al. Guardant360 circulating tumor DNA assay is concordant with FoundationOne next-generation sequencing in detecting actionable driver mutations in Anti-EGFR naive metastatic colorectal cancer. *Oncologist* **25**, 235–243 (2020).
- Rostami-Hodjegan, A., Achour, B. & Rothman, J.E. Methods and apparatus for quantifying protein abundance in tissues via cell free ribonucleic acids in liquid biopsy. Patent No. WO2019191297 (2021).
- Rodrigues, A.D. et al. Exploring the use of serum-derived small extracellular vesicles as liquid biopsy to study the induction of hepatic cytochromes P450 and organic anion transporting polypeptides. *Clin. Pharmacol. Ther.* **110**, 248–258 (2021).
- Love, M.I., Huber, W. & Anders, S. Moderated estimation of fold change and dispersion for RNA-seq data with DESeq2. *Genome Biol.* **15**, 550 (2014).
- Lenoir, C. et al. Impact of acute inflammation on cytochromes P450 activity assessed by the Geneva cocktail. *Clin. Pharmacol. Ther.* **109**, 1668–1676 (2021).
- Bosilkovska, M. et al. Simultaneous LC–MS/MS quantification of P-glycoprotein and cytochrome P450 probe substrates and their metabolites in DBS and plasma. *Bioanalysis* **6**, 151–164 (2014).
- Broccanello, C., Gerace, L. & Stevanato, P. QuantStudio™ 12K Flex OpenArray® system as a tool for high-throughput genotyping and gene expression analysis. *Methods Mol. Biol.* **2065**, 199–208 (2020).
- Barbarino, J.M., Whirl-Carrillo, M., Altman, R.B. & Klein, T.E. PharmGKB: a worldwide resource for pharmacogenomic information. *Wiley Interdiscip. Rev. Syst. Biol. Med.* **10**, e1417 (2018).
- Walsky, R.L., Astuccio, A.V. & Obach, R.S. Evaluation of 227 drugs for in vitro inhibition of cytochrome P450 2B6. *J. Clin. Pharmacol.* **46**, 1426–1438 (2006).
- Gonzalez, D. et al. Precision dosing: public health need, proposed framework, and anticipated impact. *Clin. Transl. Sci.* **10**, 443–454 (2017).
- US FDA. *Enhancing the diversity of clinical trial populations—eligibility criteria, enrollment practices, and trial designs guidance for industry* <<https://www.fda.gov/media/127712/download>> (2020).
- Wegler, C. et al. Proteomics-informed prediction of rosuvastatin plasma profiles in patients with a wide range of body weight. *Clin. Pharmacol. Ther.* **109**, 762–771 (2021).
- Rodrigues, D. & Rowland, A. From endogenous compounds as biomarkers to plasma-derived nanovesicles as liquid biopsy; has

- the golden age of translational pharmacokinetics-absorption, distribution, metabolism, excretion-drug–drug interaction science finally arrived? *Clin. Pharmacol. Ther.* **105**, 1407–1420 (2019).
22. Leopold, J.A. & Loscalzo, J. Emerging role of precision medicine in cardiovascular disease. *Circ. Res.* **122**, 1302–1315 (2018).
  23. Barber, J., Russell, M.R., Rostami-Hodjegan, A. & Achour, B. Characterization of CYP2B6 K262R allelic variants by quantitative allele-specific proteomics using a QconCAT standard. *J. Pharm. Biomed. Anal.* **178**, 112901 (2020).
  24. Klein, K. & Zanger, U.M. Pharmacogenomics of cytochrome P450 3A4: recent progress toward the ‘missing heritability’ problem. *Front. Genet.* **4**, 12 (2013).
  25. Taylor, D.D. & Gercel-Taylor, C. MicroRNA signatures of tumor-derived exosomes as diagnostic biomarkers of ovarian cancer. *Gynecol. Oncol.* **110**, 13–21 (2008).
  26. Matsumoto, Y. *et al.* Quantification of plasma exosome is a potential prognostic marker for esophageal squamous cell carcinoma. *Oncol. Rep.* **36**, 2535–2543 (2016).
  27. Silva, J. *et al.* Analysis of exosome release and its prognostic value in human colorectal cancer. *Genes Chromosom. Cancer* **51**, 409–418 (2012).
  28. Polasek, T.M. & Rostami-Hodjegan, A. Virtual twins: understanding the data required for model-informed precision dosing. *Clin. Pharmacol. Ther.* **107**, 742–745 (2020).
  29. Guest, E.J. *et al.* Assessment of algorithms for predicting drug–drug interactions via inhibition mechanisms: comparison of dynamic and static models. *Br. J. Clin. Pharmacol.* **71**, 72–87 (2011).
  30. Dunvald, A.D., Järvinen, E., Mortensen, C. & Stage, T.B. Clinical and molecular perspectives on inflammation-mediated regulation of drug metabolism and transport. *Clin. Pharmacol. Ther.* <https://doi.org/10.1002/cpt.2432>. [e-pub ahead of print].